

Reactions of the Phthalimide *N*-Oxyl Radical (PINO) with Activated Phenols: The Contribution of π -Stacking Interactions to Hydrogen Atom Transfer Rates

Claudio D'Alfonso,[†] Massimo Bietti,^{*,‡} Gino A. DiLabio,^{*,§,||} Osvaldo Lanzalunga,^{*,†} and Michela Salamone[‡]

[†]Dipartimento di Chimica, Sapienza Università di Roma and Istituto CNR di Metodologie Chimiche (IMC–CNR), Sezione Meccanismi di Reazione, c/o Dipartimento di Chimica, Sapienza Università di Roma, P.le A. Moro, 5 I-00185 Rome, Italy

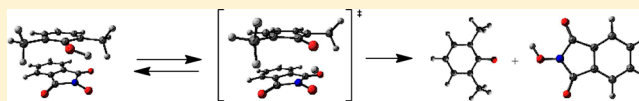
[‡]Dipartimento di Scienze e Tecnologie Chimiche, Università "Tor Vergata", Via della Ricerca Scientifica, 1 I-00133 Rome, Italy

[§]National Institute for Nanotechnology, National Research Council of Canada, 11421 Saskatchewan Drive, Edmonton, Alberta, Canada T6G 2M9

^{||}Department of Physics, University of Alberta, Edmonton, Alberta, Canada

Supporting Information

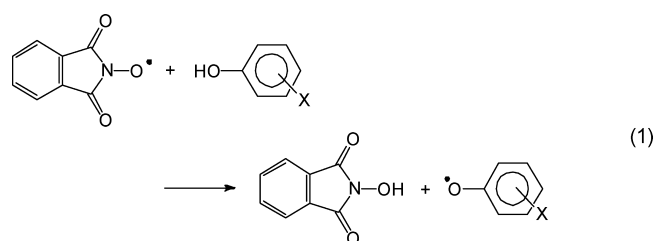
ABSTRACT: The kinetics of reactions of the phthalimide *N*-oxyl radical (PINO) with a series of activated phenols (2,2,5,7,8-pentamethylchroman-6-ol (PMC), 2,6-dimethyl- and 2,6-di-*tert*-butyl-4-substituted phenols) were investigated by laser flash photolysis in CH₃CN and PhCl in order to establish if the reactions with PINO can provide a useful tool for evaluating the radical scavenging ability of phenolic antioxidants. On the basis of the small values of deuterium kinetic isotope effects, the relatively high and negative ρ values in the Hammett correlations and the results of theoretical calculations, we suggest that these reactions proceed by a hydrogen atom transfer (HAT) mechanism having a significant degree of charge transfer resulting from a π -stacked conformation between PINO and the aromatic ring of the phenols. Kinetic solvent effects were analyzed in detail for the hydrogen transfer from 2,4,6-trimethylphenol to PINO and the data obtained are in accordance with the Snelgrove-Ingold equation for HAT. Experimental rate constants for the reactions of PINO with activated phenols are in accordance with those predicted by applying the Marcus cross relation.



INTRODUCTION

The reactivity of the phthalimide-*N*-oxyl radical (PINO) is receiving continuous attention since this species is the active oxidant in the synthetically useful *N*-hydroxyphthalimide (NHPI) catalyzed oxidation of aliphatic and alkylaromatic hydrocarbons.^{1,2} Moreover, PINO and other short-lived aminoxyl radicals play a key role in the oxidative degradation of lignin promoted by the laccase/O₂ system mediated by NHPI and other hydroxylamines,³ a process that has application in the pulp and paper industry.⁴ This interest has stimulated several studies aimed at assessing the mechanism of the reactions of these radicals with a wide variety of organic compounds. In particular, the reactivity of PINO toward C–H bonds has been investigated in detail and a classical hydrogen atom transfer (HAT) mechanism has been suggested to be operative in these processes.^{5–8} In contrast, only a few studies are available concerning the reactivity of PINO with phenolic OH groups, which leads to the formation of phenoxyl radicals (eq 1).^{9,10}

This process is of great interest for the fact that reaction 1 can play an important role in the already mentioned NHPI-mediated oxidative degradation of the abundant phenolic residues of lignin promoted by the laccase/O₂ system. More importantly, in a previous study⁹ we proposed the analysis of



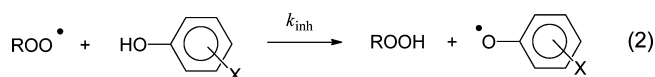
the PINO reactivity with phenols as a tool for evaluating the radical scavenging ability of phenolic antioxidants.

The antioxidant activity of phenols is based on their ability to transfer the phenolic hydrogen to lipid peroxy radicals (eq 2) much faster than the chain-propagating H-atom transfer step of lipid peroxidation (eq 3).¹¹

The rate constant for eq 2 (k_{inh}) represents a key element in the evaluation of the antioxidant properties of phenolic compounds. Its magnitude depends on several factors and in particular on the bond dissociation energy (BDE) of the phenolic O–H bond.¹² In this respect it has to be remarked that the BDE of the O–H bond of NHPI formed after

Received: November 13, 2012

Published: January 4, 2013



hydrogen abstraction by PINO (88 kcal/mol)¹⁰ is very close to that of the O–H bonds formed by alkylperoxyl radicals (89 kcal/mol for *t*BuOO–H).¹³ Thus, when considering the enthalpic effects of reactions 1 and 2, it appears that PINO may represent a good model for alkylperoxyl radicals in hydrogen transfer processes. However, as will be discussed later, other factors like polar and steric effects are at play in these processes^{2,6,12} and should be taken into account when comparing the reactivity of these two classes of oxygen-centered radicals.

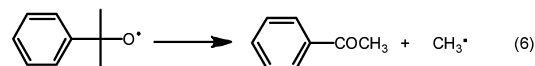
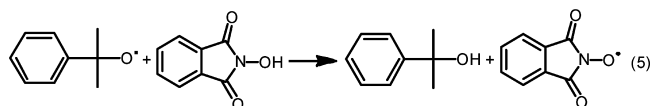
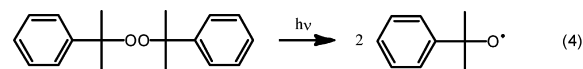
In our previous study,⁹ we performed a spectrophotometric analysis of the reaction of PINO with a series of *para*-substituted phenols (4-X-C₆H₄OH, X = H, CO₂Et, CONH₂, CH₂CN, CH₂OH, CH₃). Because these substrates have BDEs that are somewhat higher than those of typical phenolic antioxidants (*viz.* > ca. 86 kcal/mol),¹⁴ we considered it worthwhile to extend the analysis of the reaction 1 to a series of more activated phenolic compounds, namely 2,6-dimethyl-4-substituted phenols (1–5), 2,6-di-*tert*-butyl-4-substituted phenols (6–10) and 2,2,5,7,8-pentamethylchroman-6-ol (PMC, 11), whose structures are displayed in Chart 1.

Since the reaction of PINO with activated phenols is too fast to be followed by conventional spectrophotometry, the reaction kinetics were investigated by the laser flash photolysis (LFP) technique. In order to have information on the solvent effect on hydrogen abstraction from all the phenols, experiments were performed in CH₃CN and in chlorobenzene (PhCl). With 2,4,6-trimethylphenol (3), an extended series of solvents was used. We also studied the reactions of PINO with phenols 1, 4 and 5 using density-functional theory (DFT) techniques in order to develop deeper insight into the energetics and dynamics of the hydrogen transfer process between these species.

RESULTS

Time-resolved Studies. In the LFP experiments, PINO was produced after hydrogen atom abstraction from NHPI by the cumyloxyl radical (eq 5 in Scheme 1).¹⁵ The latter species was generated by 355 nm LFP of dicumyl peroxide (eq 4 in Scheme 1). The hydrogen atom transfer from NHPI to the cumyloxyl radical occurs in competition with β -scission in the

Scheme 1



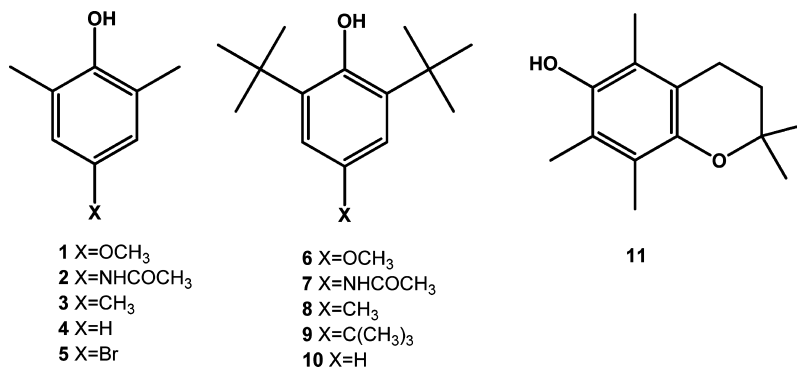
radical, which leads to the formation of acetophenone and a methyl radical (eq 6 in Scheme 1, $k_\beta \approx 6.5 \times 10^5 \text{ s}^{-1}$ in CH₃CN).¹⁶

The PINO signal, which is characterized by an absorption band centered at 380 nm,⁵ is stable on the millisecond time scale. However, in the presence of an excess of phenolic compounds,¹⁷ there occurs a fast decay that follows first order kinetics. With the exception of PMC (11), we observed no transient signals at ca. 380–400 nm that could be assigned to phenoxyl radicals.¹⁸ This observation can be reasonably explained by considering that the rate of hydrogen abstraction from the O–H group of compounds 1–10 by PINO (eq 7 in Scheme 2) is significantly lower than the rate of combination of the phenoxyl radicals with PINO (eq 8 in Scheme 2).¹⁹ The latter process, as already shown in a previous study using 2-*tert*-butyl-4-methylphenol as a substrate,⁹ led to the formation of the cross-coupling product of the two radicals (Scheme 2, R = *t*Bu, R' = H, R'' = CH₃).

The fast hydrogen abstraction from PMC (11) by PINO enables us to observe the decay of PINO along with the formation of the PMC phenoxyl radical. Figure 1 shows the time-resolved spectra obtained after 355 nm LFP of an N₂-saturated CH₂Cl₂ solution containing dicumyl peroxide (0.8 M), NHPI (5.0 mM) and PMC (0.1 mM) at *T* = 25 °C.

The PINO radical, monitored at 380 nm, undergoes a first-order decay (Figure 1, inset a) accompanied by the formation of the PMC phenoxyl radical (Figure 1, inset b) which displays the characteristic visible absorption band at $\lambda_{\text{max}} = 425 \text{ nm}$.²⁰ It can be noted that the latter radical is in part already formed 0.65 μs after the laser pulse. This can be attributed to the direct reaction of the cumyloxyl radical with PMC which occurs in competition with hydrogen transfer from NHPI²¹ despite a PMC concentration that is 50 times lower than that of NHPI.

Chart 1



Scheme 2

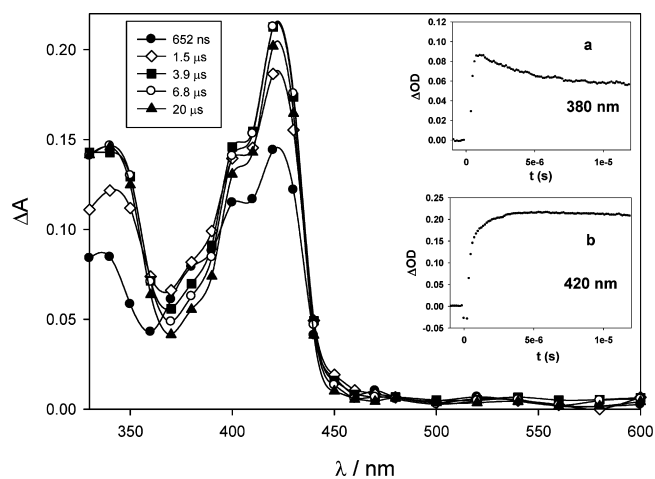
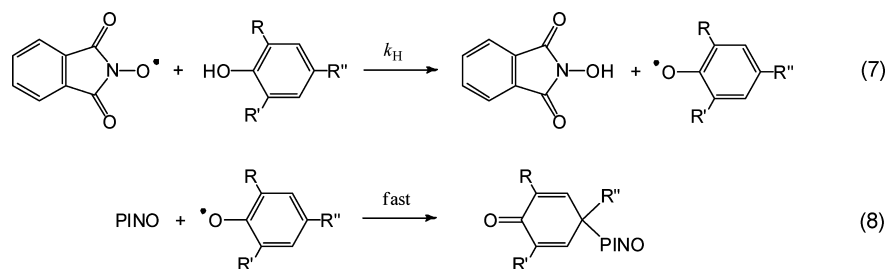


Figure 1. Time-resolved absorption spectra observed after 355 nm LFP of an N_2 -saturated CH_2Cl_2 solution ($T = 25\text{ }^\circ\text{C}$) containing dicumyl peroxide (0.8 M), NHPI (5 mM) and PMC (0.1 mM), at 652 ns (filled circles), 1.5 μs (empty diamonds), 3.9 μs (filled squares), 6.8 μs (empty circles) and 20 μs (filled triangles) after the 8 ns, 20 mJ laser flash. (Inset a) Decay of the absorption of PINO at 380 nm. (Inset b) Buildup of the absorption of the PMC phenoxyl radical at 420 nm.

When the pseudo first-order rate constants (k_{obs}) for the decay of the PINO radical measured at 380 nm were plotted against the concentration of phenolic compounds, excellent linear dependencies were observed (see Figure 2 (MeCN) and Figure S1 in the Supporting Information (PhCl) for 2,6-dimethyl-4-substituted phenols; Figure 3 (MeCN) and Figure S2 in the Supporting Information (PhCl) for 2,6-di-*tert*-butyl-4-substituted phenols). According to Scheme 2, the second-order rate constants for abstraction of the phenolic O–H hydrogen by PINO (k_{H}) were obtained from the slopes of these plots using eq 9 for the reactions with phenols 1–10 ($k_{\text{obs}} = k_{\text{H}}[\text{PMC}]$ for the reaction of PINO with PMC). The hydrogen abstraction rate constants k_{H} are reported in Table 1.

$$k_{\text{obs}} = 2k_{\text{H}}[\text{ArOH}] \quad (9)$$

The addition of 1% D_2O to CH_3CN solutions containing the more reactive methoxylated phenols 1, 6 and 11, quantitatively converts ArOH to ArOD and results in a substantial decrease in the decay rate of PINO (see Table 1, Figure 4 for the reaction of PINO with 1, Figures S3–S4 in the Supporting Information for the reactions of PINO with 6 and 11). The kinetic deuterium isotope effects ($k_{\text{H}}/k_{\text{D}}$) are 2.1, 3.1, and 1.4 respectively for phenols 1, 6 and 11.

Theoretical Calculations. We performed density-functional theory calculations to model the reactions between PINO and phenols 1, 4 and 5 in order to develop a more

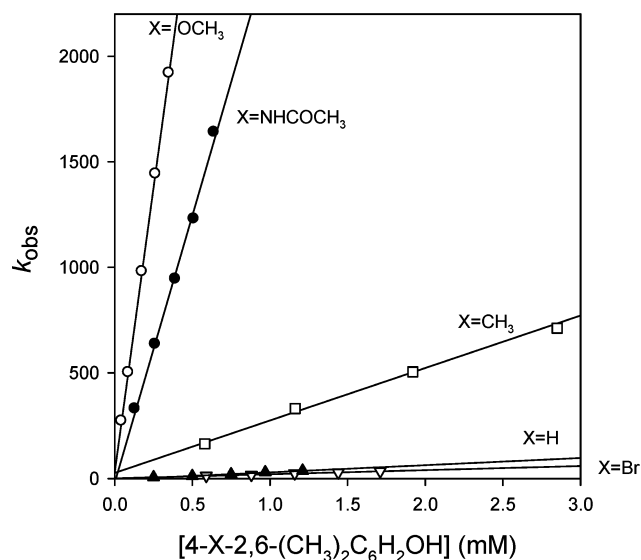


Figure 2. Dependence of k_{obs} for the decay of the PINO radical measured at 380 nm on the concentration of 4-*X*-2,6- $(CH_3)_2C_6H_2OH$ ($X = OCH_3, NHCOCH_3, CH_3, H, Br$) in CH_3CN at $25\text{ }^\circ\text{C}$.

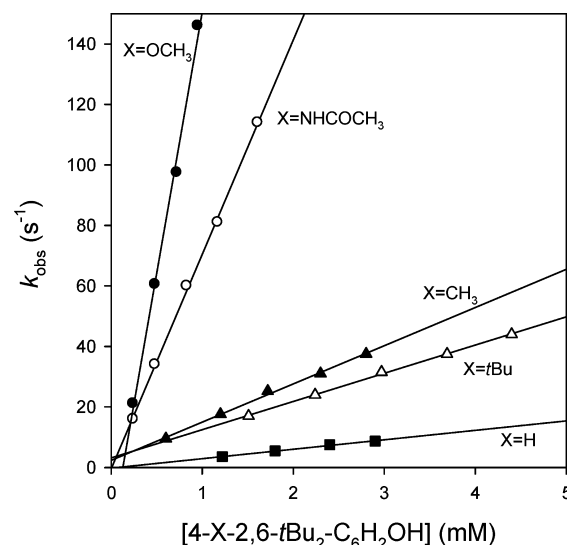
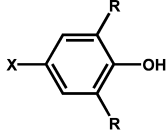


Figure 3. Dependence of k_{obs} for the decay of the PINO radical measured at 380 nm on the concentration of 4-*X*-2,6-*t*- $Bu_2C_6H_2OH$ ($X = OCH_3, NHCOCH_3, CH_3, tBu, H$) in CH_3CN at $25\text{ }^\circ\text{C}$.

detailed understanding of the hydrogen exchanges involving these species. Noncovalent interactions between the reactants are expected to play an important role in the formation of pre-reaction complexes and may influence reaction mechanism through the stabilization of the transition state complexes. In

Table 1. Second-Order Rate Constants k_{H} ($\text{M}^{-1}\text{s}^{-1}$) for the Reaction of the PINO Radical with Phenols 1–11 at 25 °C and Phenolic O–H Bond Dissociation Energies


	k_{H}	Solvent	BDE (kcal mol^{-1}) ^a
1 R = CH ₃ , X = OCH ₃	2.7 ± 0.1 × 10 ⁶	MeCN	79.7 ^b
	2.25 × 10 ⁶	MeCN + 1% H ₂ O	
	1.05 × 10 ⁶	MeCN + 1% D ₂ O	
2 R = CH ₃ , X = AcNH	1.4 ± 0.3 × 10 ⁷	PhCl	
	1.2 ± 0.2 × 10 ⁶	MeCN	
3 R = CH ₃ , X = CH ₃	1.4 ± 0.4 × 10 ⁵	MeCN	82.73
	8.0 ± 0.5 × 10 ⁵	PhOCH ₃	
	1.8 ± 0.2 × 10 ⁶	PhCl	
4 R = CH ₃ , X = H	1.9 ± 0.3 × 10 ⁶	CH ₂ Cl ₂	84.5
	1.6 ± 0.1 × 10 ⁴	MeCN	
	2.1 ± 0.3 × 10 ⁵	PhCl	
5 R = CH ₃ , X = Br	1.0 ± 0.1 × 10 ⁴	MeCN	85.0 ^c
	2.5 ± 0.6 × 10 ⁵	PhCl	
	8.0 ± 0.9 × 10 ⁴	MeCN	
6 R = <i>t</i> Bu, X = OCH ₃	7.0 × 10 ⁴	MeCN + 1% H ₂ O	78.31
	2.3 × 10 ⁴	MeCN + 1% D ₂ O	
	4.9 ± 0.5 × 10 ⁵	PhCl	
	3.6 ± 0.2 × 10 ⁴	MeCN	
7 R = <i>t</i> Bu, X = AcNH	1.7 ± 0.1 × 10 ⁵	PhCl	
	6.0 ± 0.8 × 10 ³	MeCN	
8 R = <i>t</i> Bu, X = CH ₃	3.8 ± 0.6 × 10 ⁴	PhCl	81.02
	4.8 ± 0.3 × 10 ³	MeCN	
9 R = <i>t</i> Bu, X = <i>t</i> Bu	2.8 ± 0.1 × 10 ⁴	PhCl	81.24
	8.0 ± 0.8 × 10 ³	MeCN	
10 R = <i>t</i> Bu, X = H	1.5 ± 0.1 × 10 ³	MeCN	82.8
	8.0 ± 0.8 × 10 ³	PhCl	
	2.5 ± 0.4 × 10 ⁸	CH ₃ CN	
11 PMC	2.3 × 10 ⁸	MeCN + 1% H ₂ O	78.25
	1.6 × 10 ⁸	MeCN + 1% D ₂ O	
	2.2 × 10 ⁸	MeCN + Mg(ClO ₄) ₂ 0.1 M	
	5.2 ± 0.7 × 10 ⁸	PhCl	

^aFrom ref 24. ^bCalculated using the group additivity rule with substituent contributions reported in ref 25. ^cCalculated using the group additivity rules with a contribution of ΔBDE for the *p*-Br of 0.86 kcal/mol (from ref 26).

order to ensure that we adequately model noncovalent interactions, we used the latest generation of dispersion-correcting potentials (DCPs) recently described by Torres and DiLabio,²⁷ in conjunction with B3²⁸LYP²⁹/6-31+G(2d,2p).^{30,31}

We began our simulations by attempting to quantify the binding energy differences between cisoid- and transoid-type prereaction complex structures involving PINO and phenols 1, 4, and 5. We define a cisoid structure as having the reactants arranged in a π -stacked conformation and a transoid structure as having a nearly planar conformation. The structural details of the transoid prereaction complex appear to be dependent upon substituent in the 4-position of the phenol. For example, phenols 1 and 5 were found to form planar transoid prereaction complexes with PINO, whereas phenol 4 forms no transoid structure at all and optimized along a shallow potential energy surface to the cisoid prereaction complex.

Transition state (TS) structures were explored starting from the minima associated with the prereaction complexes. Determining cisoid TSs was relatively straightforward, however

finding transoid TSs was more challenging. In fact, we were not able to locate TS structures in which the reactants were coplanar. Rather, the TSs for the PINO + 1 and PINO + 5 reactions were found to be pseudotransoid, in which there is a ca. 45° angle between the ring planes of the reactants (see Figure 5d). This indicates that the nearly planar transoid prereaction complexes must move out of plane in order to reach a pseudotransoid TS. In any case, the nature of the transoid-type prereaction complexes and TSs have little relevance to the reaction kinetics as they lie significantly higher in energy than their cisoid counterparts (see Table 2).

The relative energies/free energies associated with the reaction of PINO with phenols 1, 4, and 5 are listed in Table 2. The energy-optimized prereaction and TS complexes for the reaction of PINO with 1 are presented in Figure 5.

The data in Table 2 show that the cisoid prereaction complexes have binding energies that are almost 10 kcal/mol higher than their transoid counterparts (when formed). Cisoid binding energies range from 11.7 to 13.4 kcal/mol and both the

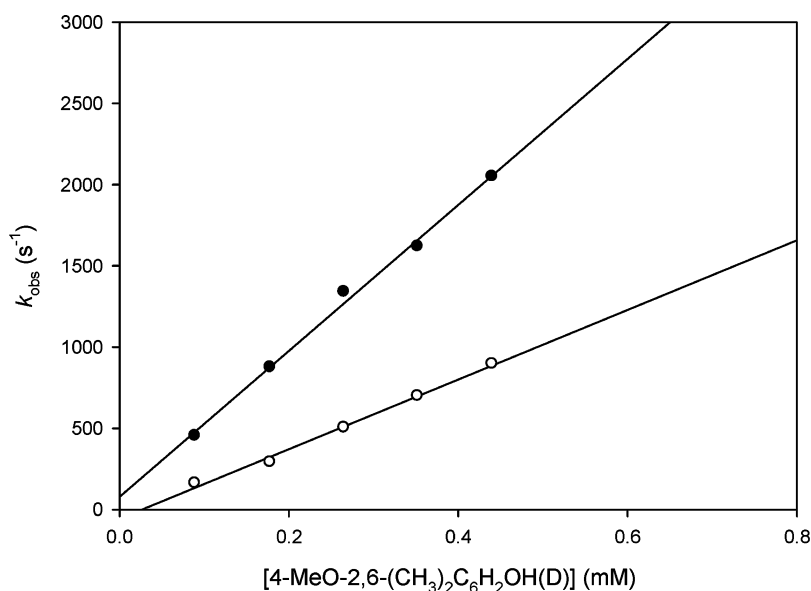


Figure 4. Dependence of k_{obs} for the decay of the PINO radical measured at 380 nm on the concentrations of 4-MeO-2,6-(CH₃)₂C₆H₂OH (●) and 4-MeO-2,6-(CH₃)₂C₆H₅OD (○) in CH₃CN + 1% H₂O (D₂O) at 25 °C.

PINO•1 and PINO•5 complexes have negative free energies of formation. The ring–ring separation between the constituents of the complexes of ca. 3.2 Å are shorter than typical π – π distances.³² The strong binding arises from attractive π -stacking interactions, along with (nonideal) hydrogen bonding between the phenol OH group and the nitroxyl moiety of PINO, and some degree of favorable interaction as a result of charge transfer from the phenol to PINO.³³

On the other hand, the transoid prereaction complexes are much more weakly bound because the single OH–O hydrogen bonding interaction has limited strength and is mitigated to some extent by steric repulsions in the vicinity of the hydrogen bond, see Figure 5c. The considerable difference in binding energies between the cisoid and transoid prereaction complexes (and, in the case of PINO•4 the complete absence of a transoid prereaction complex altogether) indicates that the latter complexes are unimportant in the kinetics of hydrogen atom transfer between phenols and PINO. This is verified by the data in Table 2, which indicate that the transoid TS structures for the PINO•1 and PINO•5 reactions are more than 3 kcal/mol higher in free energy than the corresponding cisoid TS structures.

Hydrogen atom transfer within the cisoid prereaction complexes occurs following the rotation of the OH groups of the phenols to a position ca. 90° relative to the ring plane. In the TS structures, there is little change in the separation between the rings of PINO and the phenols. Additional geometry data associated with the TS structures are provided in Figure 5 and the Supporting Information. The free energies associated with reaching the TS from separated reactants (cisoid complex) are calculated to be 4.1, 8.4, and 7.1 (4.3, 7.3, and 7.5) kcal/mol, respectively, for 1, 4, and 5. Comparisons to the data provided in Table 1 indicate that the barriers we calculated for the cisoid reactions are ca. 4 kcal/mol lower than the experimental free energy barriers in MeCN. The fact that our calculated barriers are closer to those measured in PhCl (within ca. 2.5 kcal/mol), indicates the importance of solvent effects on the calculated barriers/rate constants. Nevertheless,

there are underlying deficiencies in the B3LYP approach that contribute to the errors in calculated free energies.³⁴

DISCUSSION

From the kinetic data reported in Table 1 it can be noted that rate constants for the hydrogen abstraction (k_{H}) from phenols 1–11 by PINO span a wide range of reactivity, a difference of ca. 5 orders of magnitude is observed between the least reactive phenol 10 ($k_{\text{H}} = 1.5 \times 10^3 \text{ M}^{-1}\text{s}^{-1}$ in CH₃CN and $8.0 \times 10^3 \text{ M}^{-1}\text{s}^{-1}$ in PhCl) and the most reactive phenol 11 ($k_{\text{H}} = 2.5 \times 10^8 \text{ M}^{-1}\text{s}^{-1}$ in CH₃CN and $5.2 \times 10^8 \text{ M}^{-1}\text{s}^{-1}$ in PhCl).

The rate constants also indicate that hydrogen abstraction by PINO is significantly influenced by steric effects of the phenolic *ortho*-substituents. Accordingly, the k_{H} values for the *ortho* dimethylated phenols 1–5 are more than 1 order of magnitude higher than those observed with the *ortho* di-*tert*-butylated phenols 6–10 even though the former reactions are ca. 1.7 kcal mol⁻¹ less exothermic (see Table 1).³⁶

As was observed in our previous study of the reaction of PINO with *para*-substituted phenols,⁹ rate constants increase with the electron donating strength of the substituent in both the dimethylated phenols 1–5 and di-*tert*-butylated phenols 6–10. In accordance with the experimental data, theoretical calculations show an increase of the activation free energies, relative to the prereaction cisoid complex, from 4.3 kcal/mol for the reaction of PINO with 2,6-dimethyl-4-methoxyphenol to 7.5 kcal/mol for the reaction with 2,6-dimethyl-4-bromophenol. These results can be understood in terms of enthalpic effects by considering that electron donating (ED) groups reduce the bond dissociation enthalpy (BDE) of the phenolic O–H bonds (see Table 1) by the double effect of stabilization of the phenoxyl radical (whose O• group is strongly electron withdrawing)³⁸ and destabilization of the phenols.^{12,39}

The results of our theoretical calculations shed additional light on the dynamics of the hydrogen transfer process from phenols 1, 4, and 5 to PINO. Starting from the energetically favorable cisoid-type prereaction complex (see Figure 5a), on going to the cisoid TS, the phenolic OH group is rotated so

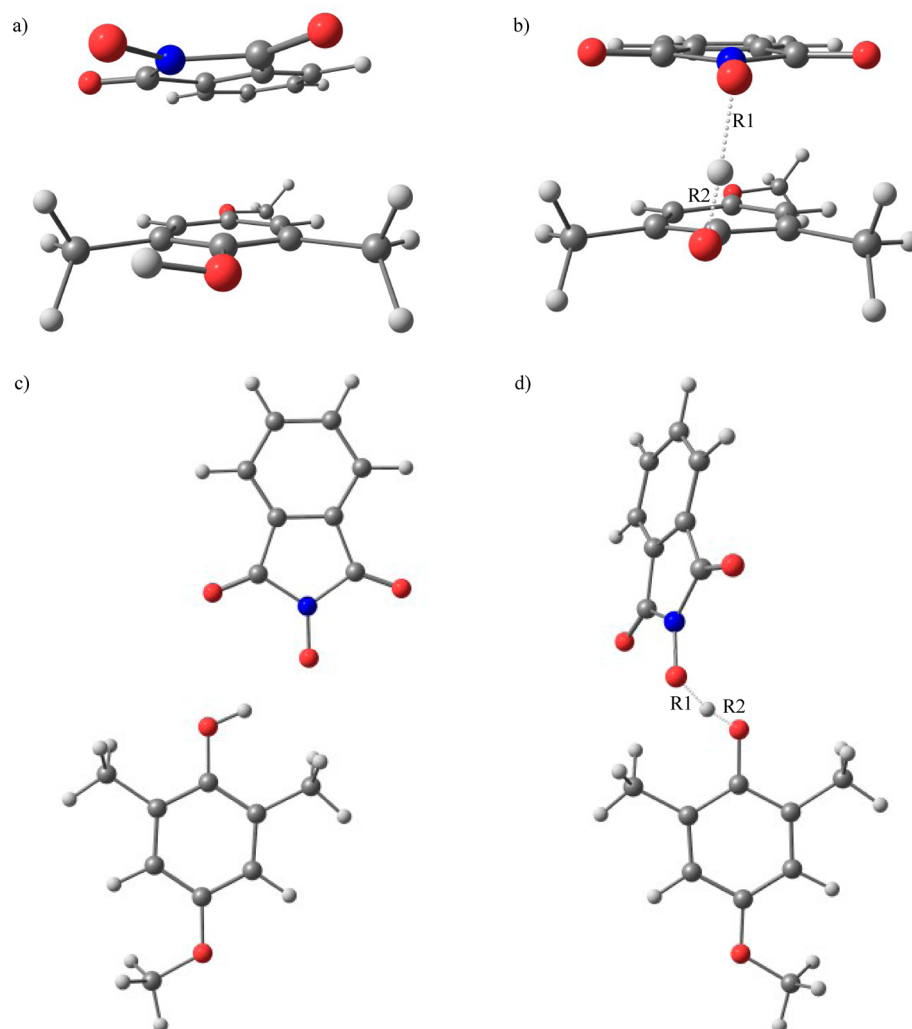


Figure 5. Prereaction complexes formed by PINO and **1** and their associated hydrogen transfer transition state complexes. (a) Cisoid (π -stacked) prereaction complex. (b) Cisoid (π -stacked) transition state structure ($R1 = 1.30 \text{ \AA}$, $R2 = 1.13 \text{ \AA}$). In both (a) and (b), the molecular planes are separated by ca. 3.2 \AA . These structures are representative of those involving **4** and **5**. (c) Transoid, coplanar prereaction complex ($R(\text{OH}\cdots\text{ON}) = 2.03 \text{ \AA}$). (d) Transoid transition state structure (nonplanar), ($R1 = 1.35 \text{ \AA}$, $R2 = 1.08 \text{ \AA}$). These structures are representative of those involving **5**. See text for additional details.

Table 2. Energies/Free Energies (kcal/mol), Relative to Reactants, for the Reactions of PINO with **1**, **4**, and **5** as Obtained from B3LYP-DCP/6-31+G(2d,2p) Calculations

reaction	structure	complex	transition state
PINO + 1	cisoid	-13.3/-0.2	-7.0/4.1
	transoid	-4.2/5.4	-1.1/7.5
PINO + 4	cisoid	-11.7/1.1	-0.7/8.4
	transoid		
PINO + 5	cisoid	-13.4/-0.4	-2.8/7.1
	transoid	-4.8/4.7	3.2/11.3

that it is pointing toward the singly occupied oxygen p-orbital of PINO (see Figure 5b). The geometry of the cisoid TS clearly indicates that a HAT process (rather than a PCET process)⁴⁰ occurs in which the proton and the electron are transferred from the phenolic O–H, along one pathway, to the singly occupied oxygen p-orbital of PINO. Figure 6, which shows the beta-spin highest molecular orbital (HOMO) for the PINO + **4** reaction, indicates the pathway associated with HAT as a

portion of an orbital showing bonding overlap between the phenol OH and the PINO singly occupied p-type orbital.

However, Figure 6 also shows that there is a bonding π – π overlap involving the phenol and PINO rings. This indicates that the π -stacking in the TS allows for some degree of charge transfer between the reacting species. The overall HAT process starting from separated reactants through the cisoid prereaction complex and the π -stacked cisoid TS is described in Scheme 3.

It has to be noted that evidence for a key role played by π -stacking interactions in the reactivity of oxygen centered radicals has also recently been proposed by our groups in the (inner sphere) electron transfer reactions from alkyl ferrocenes to benzyloxyl and cumyloxyl radicals. In this case the alkoxy radical aromatic ring can act as an electron relay shuttling the electron from the ferrocene to the formal oxygen atom radical center.⁴²

The charge transfer occurring in the HAT transition state with development of the partial positive charge on the phenolic ring is in accordance with the relatively high and negative ρ values observed when the $\log(k_{\text{H}}^{\text{X}}/k_{\text{H}}^{\text{H}})$ values for the reactions of PINO with phenols **1**–**5** and **6**–**10** in MeCN, were plotted

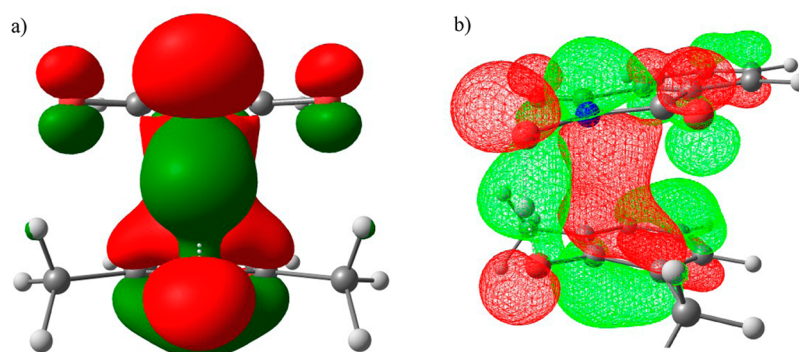


Figure 6. Two views of the highest-occupied beta molecular orbital for the transition state associated with the reaction of PINO with **4**. The view in (a) is similar to that shown in Figure 5b. Red and green represent the two different phases of the molecular orbitals.

Scheme 3

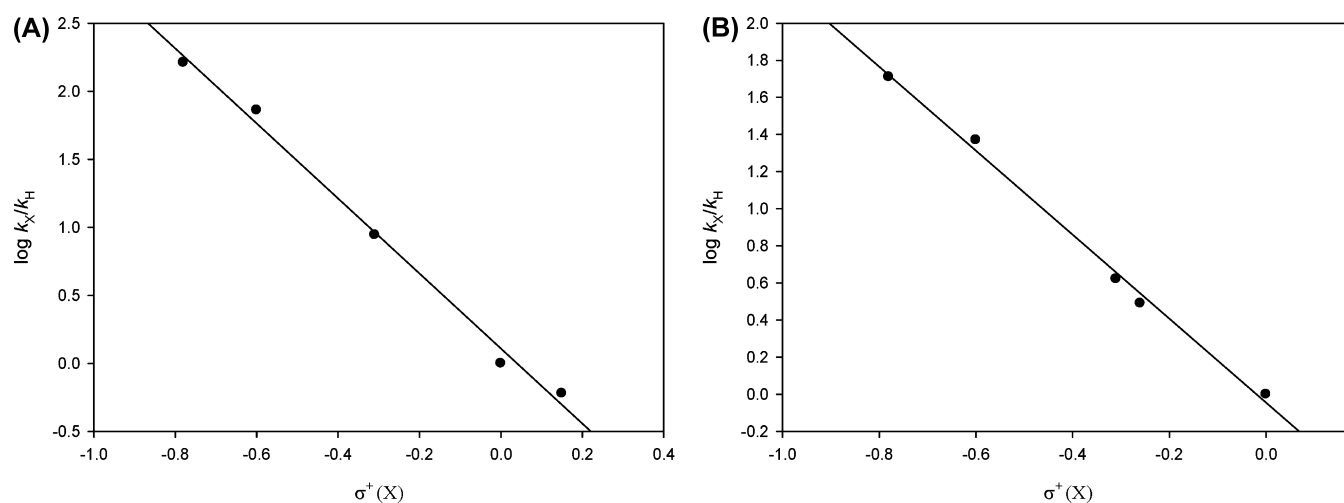
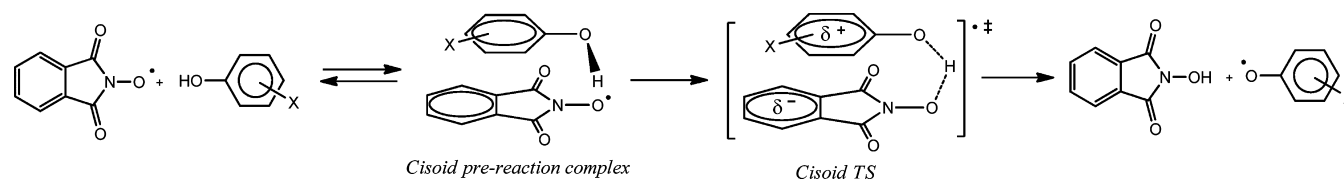


Figure 7. Hammett plots for the reactions of (A) 4-X-2,6-(CH₃)₂C₆H₂OH and (B) 4-X-2,6-*t*Bu₂C₆H₂OH with PINO in CH₃CN at 25 °C.

against the substituent constants σ^+ . The excellent Hammett correlations thus obtained are shown in Figure 7.

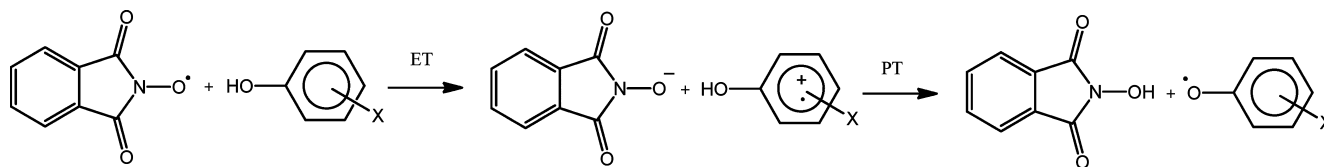
It is interesting to note that the ρ values for the *ortho*-dimethylated (-2.76) and *ortho*-di-*tert*-butylated phenols (-2.26) are much more negative than those found in the reaction of the two series of phenols with the styrylperoxyl radical (-1.36 and -1.11 , respectively).⁴³ This result can be likely attributed to the greater development of positive charge in the phenolic ring in the TS of the hydrogen abstraction promoted by the PINO with respect to the styrylperoxyl radical deriving from the charge transfer contribution from the π -stacked conformation (see later).

It is also interesting to compare the ρ values for the *ortho*-dimethylated and *ortho*-di-*tert*-butylated phenols with that previously determined in the reaction of PINO with the *para*-substituted phenols ($\rho = -3.1$).⁹ The electronic effect of the substituent is somewhat reduced in the presence of the 2,6-dialkyl substituents. This observation is in accordance with a lower degree of CT in the earlier TS for the HAT process from

the *ortho*-dialkyl substituted phenols. The less negative ρ value found in the 4-X-2,6-*t*Bu₂C₆H₂OH series with respect to the 4-X-2,6-(CH₃)₂C₆H₂OH one probably reflects the smaller extent of CT that occurs in the TS due to the bulkiness of the *ortho* alkyl groups.

For the more reactive phenols **1**, **6** and **11** it was possible to analyze the kinetic deuterium isotope effect (DKIE) by LFP experiments. The observation of a decrease in the decay rate of PINO by replacing ArOH with ArOD is in accordance with a fast formation of the cisoid prereaction complex followed by a rate determining HAT reaction (Scheme 3). As previously reported for the reaction of PINO with *para*-substituted phenols,⁹ the DKIE values are not very high ($k_H/k_D = 2.1$, 3.1, and 1.4 for **1**, **6** and **11** respectively) in line with a nonsymmetrical transition state for the highly exothermic hydrogen transfer process ($\Delta H = -8.2$, -9.8 , and -9.9 kcal mol⁻¹ for the reaction of PINO with **1**, **6** and **11** respectively).⁴⁴ This hypothesis is supported by the results of theoretical calculations, for example in the cisoid TS for the

Scheme 4



reaction of PINO with **1** the distance of the H from the phenolic O (1.13 Å) is much shorter than the H distance from the PINO oxygen (1.30 Å) (see Figure 5). The slightly higher DKIE value found in the reaction of PINO with **6** might be attributed to the steric effect due to the encumbrance of the two *ortho tert*-butyl substituents that causes an increase of the degree of hydrogen transfer from the phenolic O–H to the PINO radical in the TS.

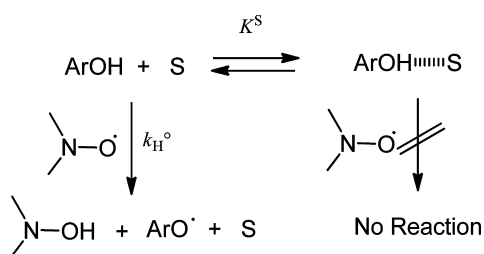
Even though PINO and other short-lived aminoxyl radicals are good one-electron oxidants^{23,45} the possibility that the hydrogen abstraction reaction proceeds by a two step electron transfer-proton transfer process (Scheme 4) as in the *N*-demethylation of *N,N*-dimethylanilines^{15a,46} instead of a HAT mechanism, is unlikely. The ET-PT mechanism with a rate-determining ET would not be in accordance with the DKIEs observed. Moreover such an ET process would be endergonic as the reduction potential of PINO in CH₃CN is 0.69 V vs SCE²³ while the oxidation potential of the phenols investigated are ≥0.97 V vs. SCE in CH₃CN (E_{ox}° for PMC, the most easily oxidizable phenol investigated in this study).^{47,48}

Since it has been reported that the effect of Mg²⁺ on hydrogen transfer rates can provide a reliable criterion for distinguishing between the one-step HAT and the ET mechanisms,^{20,49} we also investigated the effect of Mg²⁺ on the oxidation reaction of PMC. No variation in the rate constant for hydrogen transfer from PMC to PINO was observed after addition of Mg(ClO₄)₂ 0.1 M (Table 1), thus providing additional support to the hypothesis that the reaction proceeds via a one-step HAT rather than via ET.

In order to investigate the kinetic solvent effect (KSE) on the HAT process from the phenols to PINO, rate constants were also determined in PhCl for phenols **1–10** and in a more extended series of solvents (CH₂Cl₂, PhCl, PhOMe, MeCN) for 2,4,6-trimethylphenol (**3**).⁵⁰ From the k_{H} values reported in Table 1 it can be easily noted that the reactivity depends on the hydrogen bond accepting ability of the solvent, as measured by the Abraham's β_2^{H} values.⁵¹ The lower the β_2^{H} value, the higher the reactivity of phenols with PINO. These findings are in agreement with Ingold's model for HAT processes reported in Scheme 5.^{22,52}

In Scheme 5, k_{H}° represents the rate constant measured in a non-HBA solvent (i.e., an alkane for which $\beta_2^{\text{H}} = 0.00$) and K^{S} is the equilibrium constant for hydrogen bond formation

Scheme 5



between phenol and solvent S. According to this picture, in relatively strong HBA solvents the substrate must experience desolvation in order to undergo hydrogen abstraction and a decrease in reactivity is observed as compared to weaker or non-HBA solvents. In general, the rate constant for hydrogen abstraction from phenol in a solvent S, k_{H}^{S} , can be expressed in terms of eq 10.

$$k_{\text{H}}^{\text{S}} = k_{\text{H}}^{\circ} / (1 + K^{\text{S}}[\text{S}]) \quad (10)$$

The Snelgrove–Ingold empirical equation (eq 11)^{52,53} accounts quantitatively for the KSEs observed in these reactions.

$$\log(k_{\text{H}}^{\text{S}}) = \log(k_{\text{H}}^{\circ}) - 8.3\alpha_2^{\text{H}}(\text{subst})\beta_2^{\text{H}} \quad (11)$$

In this equation, $\alpha_2^{\text{H}}(\text{subst})$ measures the substrate hydrogen bond donor (HBD) ability.⁵⁴ When the $\log k_{\text{H}}$ values for the reactions of phenol **3** with PINO in the four solvents investigated were plotted against the solvent β_2^{H} values, a good correlation was obtained (Figure 8).

From the linear regression analysis an intercept of 6.5 is obtained, therefore in a non-HBA solvent (e.g., alkane solvents) the k_{H} for the reaction between the PINO radical and 2,4,6-trimethylphenol can be estimated as ca. $3.2 \times 10^6 \text{ M}^{-1}\text{s}^{-1}$. In accordance with the prediction of the Snelgrove–Ingold equation the slope of the plot of Figure 8 (–2.9) is very close to the product $-8.3\alpha_2^{\text{H}}(\text{subst})$ (–3.1 using $\alpha_2^{\text{H}} = 0.374$ for 2,4,6-trimethylphenol^{52a}).

The relevant contribution of charge transfer in the reaction of PINO with activated phenols is highlighted by the comparison of the rate constants for reaction of PINO with PMC with those reported in the literature for the hydrogen abstraction from α -tocopherol by the cumylperoxy radical (Table 3).⁵⁵ The latter process likely occurs by a mechanism involving PCET, wherein a proton is transferred between O atoms and an electron transferred via a peroxy oxygen lone pair-phenolic ring π overlap.⁵⁶

The data reported in Table 3 indicate that PINO is at least 2 orders of magnitude more reactive than CumOO• in hydrogen transfer processes from O–H bonds in activated phenols.

The higher reactivity of PINO with respect to alkylperoxy radicals has been observed in several HAT processes from C–H bonds and rationalized on the basis of the more significant polar effects in the reactions promoted by PINO.^{2,6} The higher PINO vs ROO• relative reactivity found in hydrogen abstraction from phenolic O–H bonds than from C–H bonds can be likely attributed to the fact that the former HAT is facilitated by the greater orbital overlap that occurs in the π -stacked conformation compared to lone pair π overlaps.

Lastly, we compared the experimental rate constants for the reactions of PINO with phenols with those calculated by applying the Marcus cross relation. As recently reviewed by Mayer,⁵⁷ the Marcus cross relation accurately predicts rate constants for a large number of organic and transition metal HAT reactions, including substrates with C–H, N–H, and O–

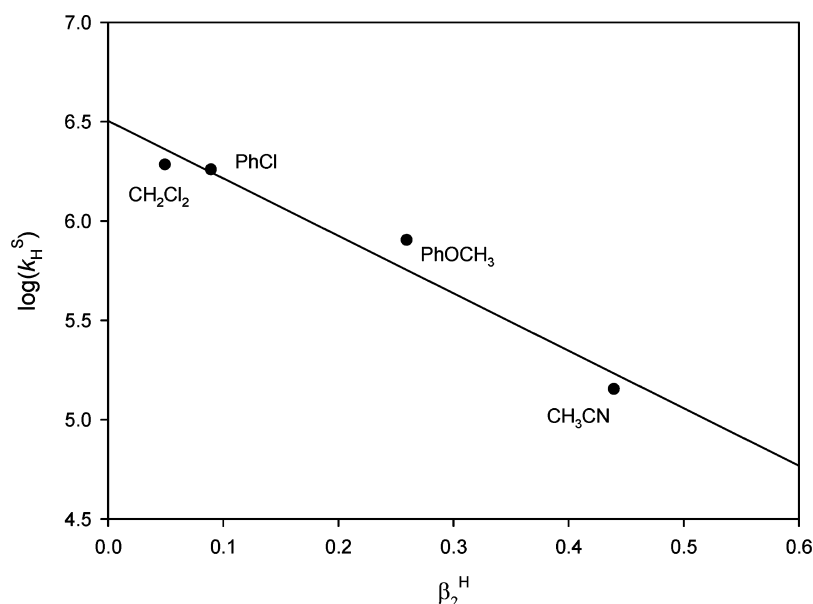


Figure 8. Plot of $\log k_{\text{H}}$ vs solvent β_2^{H} value for the reactions between the PINO radical and 2,4,6-trimethylphenol (3). From the linear regression analysis: intercept = 6.5, slope = -2.9 , $r^2 = 0.958$.

Table 3. Second Order Rate Constants (k_{H} , $\text{M}^{-1}\text{s}^{-1}$) for the Hydrogen Transfer Reactions of PINO with PMC and Cumylperoxyl Radical with α -Tocopherol

solvent	k_{H}	
	PINO + PMC	CumOO* + α -Toc ^a
CH ₃ CN	2.7×10^8	3.8×10^5
PhCl	5.2×10^8	2.7×10^6

^aFrom ref 55.

H bonds in a large variety of solvents. The cross relation, as applied to HAT reactions (eq 12), predicts that HAT intrinsic barriers can be independently determined from self-exchange reactions. This derives from the “additivity postulate” that the reorganization energy λ for the cross reaction is the mean of the self-exchange λ 's (eqs 13–14).



$$\Delta G_{\text{AH/B}}^{\ddagger} = (\lambda_{\text{AH/B}}/4)(1 + \Delta G_{\text{AH/B}}^{\circ}/\lambda_{\text{AH/B}})^2 \quad (13)$$

$$\lambda_{\text{AH/B}} = (\lambda_{\text{AH/A}} + \lambda_{\text{BH/B}})/2 \quad (14)$$

Thus the rate constant for a cross reaction $k_{\text{AH/B}}$ can be calculated by applying eq 15 where $k_{\text{AH/A}}$ and $k_{\text{BH/B}}$ are the two rate constants for the respective hydrogen-atom self-exchange reactions and $K_{\text{AH/B}}$ is the equilibrium constant. The factor f is close to 1 for many of the reactions, when $|\Delta G^{\circ}| \ll 2\lambda$.⁵⁸

$$k_{\text{AH/B}} = \sqrt{k_{\text{AH/A}}k_{\text{BH/B}}k_{\text{AH/B}}/f} \quad (15)$$

In this way we calculated the hydrogen transfer rate constants for the reactions of PINO with three phenols: PMC (11), 2,6-di-*tert*-butyl-4-methoxyphenol (6) and 2,4,6-tri-*tert*-butylphenol (9), comparing the results with the experimental rate constants for the same reactions reported in Table 1. The self-exchange rate constant for the NHPI/PINO couple ($k_{\text{BH/B}}$) was derived from pseudo-self-exchange reactions in AcOH ($5 \times 10^2 \text{ M}^{-1}\text{s}^{-1}$)⁸ and it is interesting to note that the same value of $k_{\text{BH/B}}$ has been estimated for the *tert*-butylperoxyl radical ($5 \times$

$10^2 \text{ M}^{-1}\text{s}^{-1}$).⁵⁹ The self-exchange rate constants for the phenol/phenoxyl radical couples ($k_{\text{AH/A}}$) in MeCN are available in the literature⁶⁰ and are reported in Table 4. $K_{\text{AH/B}}$ were calculated

Table 4. Self Exchange Rate Constant for the Phenol/Phenoxyl Radical Couples ($k_{\text{AH/A}}$), Equilibrium Constants ($K_{\text{AH/B}}$), Experimental and Calculated Rate Constants ($k_{\text{AH/B}}$) for the HAT Reaction of PINO with Phenols 6, 9 and 11 at 25 °C in MeCN

phenol	$k_{\text{AH/A}}^a$	$K_{\text{AH/B}}$	$k_{\text{AH/B}}^a$	
			experimental	calculated
6	20	1.2×10^7	1.6×10^5	3.5×10^5
9	20	9.9×10^4	9.6×10^3	3.1×10^4
11	2.2×10^{10b}	1.4×10^7	2.7×10^8	1.2×10^7

^a $\text{M}^{-1}\text{s}^{-1}$. ^bApproximated as $k_{\text{AH/A}}$ for α -tocopherol.

from the ΔBDE values.⁴⁴ In our calculations we made the simplifying assumption that $\log K_{\text{AH/B}}$ varies approximately in proportion to the reaction heat and we assumed that $|\Delta S^{\circ}| \cong 0$ and $\Delta H^{\circ} \cong \Delta G^{\circ}$.⁶¹

Considering the approximations used in the calculation of the $k_{\text{AH/B}}$ values, the agreement between the measured rate constants with those predicted by applying the Marcus cross relation is good.

CONCLUSIONS

Kinetic analysis and theoretical calculations for the reaction of PINO with activated phenols lead to the intriguing result that this process occurs by a hydrogen atom transfer (HAT) mechanism with a contribution from charge transfer deriving from the π -stacking of the phenolic and PINO aromatic rings in a cisoid TS. The mechanism proposed is therefore different from the PCET process suggested to be operative in the reaction of alkylperoxyl radicals with phenolic antioxidants. On the basis of this difference, caution should be taken when PINO is considered a model of alkylperoxyl radicals and when the kinetic analysis of its reactions with phenolic compounds is used for evaluating the radical scavenging ability of phenolic

antioxidants. Very importantly, such charge transfer contribution from π -stacking may not be limited to HAT from phenolic O–H groups but may also play a role in the hydrogen abstraction reactions from benzylic C–H bonds. In this context, it is worth mentioning that a HAT process taking place in a charge-transfer (CT) complex was suggested to occur in reactions of substituted PINO radicals with benzylic alcohols.⁷ Important information on the role played by the π -stacking CT in the HAT reactions from phenolic O–H and benzylic C–H bonds to PINO and other short-lived aromatic aminoxyl radicals will be provided by kinetic studies and theoretical calculations which are currently being performed in our laboratories.

EXPERIMENTAL SECTION

Materials. CH₃CN, CH₂Cl₂ (spectrophotometric grade), chlorobenzene and anisole (RPE for analysis), dicumyl peroxide and *N*-hydroxyphthalimide were used as received. Phenols **1–11** are commercially available and were further purified by sublimation.

Laser Flash Photolysis Experiments. Laser flash photolysis experiments were carried out with an Applied Photophysics LK-60 laser kinetic spectrometer providing 8 ns pulses, using the third harmonic (355 nm) of a Quantel Brilliant-B Q-switched Nd:YAG laser. The laser energy was adjusted to ≤ 10 mJ/pulse by the use of the appropriate filter. A 3.5 mL Suprasil quartz cell (10 mm \times 10 mm) was used for all the experiments. N₂-saturated CH₃CN solutions of dicumyl peroxide (1 M), *N*-hydroxyphthalimide (5.0 mM) and the pertinent phenol (0.05–4.5 mM) were used. All the experiments were carried out at $T = 25 \pm 0.5$ °C under magnetic stirring. Data were collected at individual wavelengths with an Agilent Infinium oscilloscope and analyzed with the kinetic package implemented in the instrument. Rate constants were obtained by monitoring the change of absorbance at 380 nm by averaging 3–5 values. Each kinetic trace obeyed a first-order kinetic and second order rate constants were obtained from the slopes of the plots of the observed rate constants k_{obs} vs substrate concentration.

ASSOCIATED CONTENT

Supporting Information

Dependence of k_{obs} for the decay of the PINO radical on the concentrations of phenols **1–10** in PhCl and on the concentrations of phenols **6** and **11** in CH₃CN + 1% H₂O (D₂O), Cartesian coordinates of optimized structures associated with the reactions of PINO with phenols **1**, **4**, and **5**. This material is available free of charge via the Internet at <http://pubs.acs.org>.

AUTHOR INFORMATION

Corresponding Author

*E-mail: osvaldo.lanzalunga@uniroma1.it, bietti@uniroma2.it, Gino.DiLabio@nrc.ca.

Notes

The authors declare no competing financial interest.

ACKNOWLEDGMENTS

Thanks are due to the Ministero dell'Istruzione, dell'Università e della Ricerca (MIUR) and the Consiglio Nazionale delle Ricerche (CNR) for financial support, and to Westgrid for access to computational resources. We thank Prof. Lorenzo Stella for the use of a LFP equipment.

REFERENCES

(1) (a) Ishii, Y.; Nakayama, K.; Takeno, M.; Sakaguchi, S.; Iwahama, T.; Nishiyama, Y. *J. Org. Chem.* **1995**, *60*, 3934–3935. (b) Ishii, Y.;

Iwahama, T.; Sakaguchi, S.; Nakayama, K.; Nishiyama, Y. *J. Org. Chem.* **1996**, *61*, 4520–4526. (c) Yoshino, Y.; Hayashi, Y.; Iwahama, T.; Sakaguchi, S.; Ishii, Y. *J. Org. Chem.* **1997**, *62*, 6810–6813. (d) Wentzel, B. B.; Donners, M. P. J.; Alsters, P. L.; Feiters, M. C.; Nolte, R. J. M. *Tetrahedron* **2000**, *56*, 7797–7803. (e) Ishii, Y.; Sakaguchi, S.; Iwahama, T. *Adv. Synth. Catal.* **2001**, *343*, 393–427. (f) Minisci, F.; Recupero, F.; Pedulli, G. F.; Lucarini, M. *J. Mol. Catal. A* **2003**, *204–205*, 63–90. (g) Minisci, F.; Recupero, F.; Cecchetto, A.; Gambarotti, C.; Punta, C.; Paganelli, R. *Org. Proc. Res. Dev.* **2004**, *8*, 163–168. (h) Sheldon, R. A.; Arends, I. W. C. E. *Adv. Synth. Catal.* **2004**, *346*, 1051–1071. (i) Yang, G.; Ma, Y.; Xu, J. *J. Am. Chem. Soc.* **2004**, *126*, 10542–10543. (j) Yang, G.; Zhang, Q.; Miao, H.; Tong, X.; Xu, J. *Org. Lett.* **2005**, *7*, 263–266. (k) Aoki, Y.; Sakaguchi, S.; Ishii, Y. *Tetrahedron* **2006**, *62*, 2497–2500. (l) Ishii, Y.; Sakaguchi, S. *Catal. Today* **2006**, *117*, 105–113. (m) Sheldon, R. A.; Arends, I. W. C. E. *J. Mol. Catal. A* **2006**, *251*, 200–214. (n) Nechab, M.; Kumar, D. N.; Philouze, C.; Einhorn, C.; Einhorn, J. *Angew. Chem., Int. Ed.* **2007**, *46*, 3080–3083. (o) Lee, J. M.; Park, E. J.; Cho, S. H.; Chang, S. *J. Am. Chem. Soc.* **2008**, *130*, 7824–7825. (p) Yang, X.; Zhou, L.; Chen, Y.; Chen, C.; Su, Y.; Miao, H.; Xu, J. *Catal. Commun.* **2009**, *11*, 171–174. (q) Coseri, S. *Catal. Rev.* **2009**, *51*, 218–292. (r) Zheng, G.; Liu, C.; Wang, Q.; Wang, M.; Yang, G. *Adv. Synth. Catal.* **2009**, *351*, 2638–2642. (s) Yang, X.; Wang, Y.; Zhou, L.; Chen, C.; Xu, J. *J. Chem. Technol. Biotechnol.* **2010**, *85*, 564–568. (t) Melone, L.; Gambarotti, C.; Prosperini, S.; Pastori, N.; Recupero, F.; Punta, C. *Adv. Synth. Catal.* **2011**, *353*, 147–154. (u) Aguadero, A.; Falcon, H.; Campos-Martin, J. M.; Al-Zahrani, S. M.; Fierro, J. L. G.; Alonso, J. A. *Angew. Chem., Int. Ed.* **2011**, *50*, 6557–6561. (v) Lin, R.; Chen, F.; Jiao, N. *Org. Lett.* **2012**, *14*, 4158–4161. (w) Zhang, Q.; Chen, C.; Xu, J.; Wang, F.; Gao, J.; Xia, C. *Adv. Synth. Catal.* **2011**, *353*, 226–230.

(2) Recupero, F.; Punta, C. *Chem. Rev.* **2007**, *107*, 3800–3842.
(3) (a) Call, H. P.; Mücke, I. *J. Biotechnol.* **1997**, *53*, 163–202. (b) Sealey, B. J.; Ragauskas, A. J.; Elder, T. J. *Holzforchung* **1999**, *53*, 498–502. (c) Xu, F.; Kulys, J. J.; Duke, K.; Li, K.; Krikstopaitis, K.; Deussen, H.-J. W.; Abbate, E.; Galinyte, V.; Schneider, P. *Appl. Environ. Microbiol.* **2000**, *66*, 2052–2056. (d) Xu, F.; Deuss, H.-J. W.; Lopez, B.; Lam, L.; Li, K. *Eur. J. Biochem.* **2001**, *268*, 4169–4176. (e) D'Acunzo, F.; Baiocco, P.; Fabbrini, M.; Galli, C.; Gentili, P. *New J. Chem.* **2002**, *26*, 1791–1794. (f) Baiocco, P.; Barreca, A. M.; Fabbrini, M.; Galli, C.; Gentili, P. *Org. Biomol. Chem.* **2003**, *1*, 191–197. (g) Geng, X.; Li, K.; Xu, F. *Appl. Microbiol. Biotechnol.* **2004**, *64*, 493–496. (h) Annunziatini, C.; Baiocco, P.; Gerini, M. F.; Lanzalunga, O.; Sjögren, B. *J. Mol. Catal. B: Enzymatic* **2005**, *32*, 89–96. (i) Branchi, B.; Galli, C.; Gentili, P. *Org. Biomol. Chem.* **2005**, *3*, 2604–2614. (j) Astolfi, P.; Brandi, P.; Galli, C.; Gentili, P.; Gerini, M. F.; Greci, L.; Lanzalunga, O. *New J. Chem.* **2005**, *29*, 1308–1317.

(4) Argyropoulos, D. S.; Menachem, S. B. *Biotechnology in the Pulp and Paper Industry*; Eriksson, K. E. L., Ed.; Springer-Verlag: Berlin Heidelberg, 1997; pp 127–158.

(5) (a) Ueda, C.; Noyama, M.; Ohmori, H.; Masui, M. *Chem. Pharm. Bull.* **1987**, *35*, 1372–1377. (b) Minisci, F.; Punta, C.; Recupero, F.; Fontana, F.; Pedulli, G. F. *J. Org. Chem.* **2002**, *67*, 2671–2676. (c) Koshino, N.; Cai, Y.; Espenson, J. H. *J. Phys. Chem. A* **2003**, *107*, 4262–4267. (d) Hermans, I.; Vereecken, L.; Jacobs, P. A.; Peeters, J. *Chem. Commun.* **2004**, 1140–1141. (e) Brandi, P.; Galli, C.; Gentili, P. *J. Org. Chem.* **2005**, *70*, 9521–9528. (f) Hermans, I.; Jacobs, P. A.; Peeters, J. *Phys. Chem. Chem. Phys.* **2007**, *9*, 686–690. (g) Da Silva, G.; Bozzelli, J. W. *J. Phys. Chem. C* **2007**, *111*, 5760–5765. (h) Galli, C.; Gentili, P.; Lanzalunga, O. *Angew. Chem., Int. Ed.* **2008**, *47*, 4790–4796. (i) Hermans, I.; Jacobs, P. A.; Peeters, J. *Phys. Chem. Chem. Phys.* **2008**, *10*, 1125–1132. (j) Coniglio, A.; Galli, C.; Gentili, P.; Vadalà, R. *Org. Biomol. Chem.* **2009**, *7*, 155–160. (k) Sun, Y.; Zhang, W.; Hu, X.; Li, H. *J. Phys. Chem. B* **2010**, *114*, 4862–4869. (l) Chen, K.; Sun, Y.; Wang, C.; Yao, Y.; Chen, Z.; Li, H. *Phys. Chem. Chem. Phys.* **2012**, *14*, 12141–12146.

(6) Minisci, F.; Recupero, F.; Cecchetto, A.; Gambarotti, C.; Punta, C.; Faletti, R.; Paganelli, R.; Pedulli, G. F. *Eur. J. Org. Chem.* **2004**, 109–119.

- (7) Annunziatini, C.; Gerini, M. F.; Lanzalunga, O.; Lucarini, M. J. *Org. Chem.* **2004**, *69*, 3431–3438.
- (8) Cai, Y.; Koshino, N.; Saha, B.; Espenson, J. H. *J. Org. Chem.* **2005**, *70*, 238–243.
- (9) Baciocchi, E.; Gerini, M. F.; Lanzalunga, O. *J. Org. Chem.* **2004**, *69*, 8863–8866.
- (10) Amorati, R.; Lucarini, M.; Mugnaini, V.; Pedulli, G. F.; Minisci, F.; Recupero, F.; Fontana, F.; Astolfi, P.; Greci, L. *J. Org. Chem.* **2003**, *68*, 1747–1754.
- (11) (a) Burton, G. W.; Doba, T.; Gabe, E. J.; Hughes, L.; Lee, F. L.; Prasad, L.; Ingold, K. U. *J. Am. Chem. Soc.* **1985**, *107*, 7053–7065. (b) Burton, G. W.; Ingold, K. U. *Acc. Chem. Res.* **1986**, *19*, 194–201. (c) Valgimigli, L.; Lucarini, M.; Pedulli, G. F.; Ingold, K. U. *J. Am. Chem. Soc.* **1997**, *119*, 8095–8096.
- (12) (a) Denisov, E. T.; Khudryakov, I. V. *Chem. Rev.* **1987**, *87*, 1313–1357. (b) Amorati, R.; Ferroni, F.; Pedulli, G. F.; Valgimigli, L. *J. Org. Chem.* **2003**, *68*, 9654–9658. (c) Mulder, P.; Korth, H.-G.; Pratt, D. A.; DiLabio, G. A.; Valgimigli, L.; Pedulli, G. F.; Ingold, K. U. *J. Phys. Chem. A* **2005**, *109*, 2647–2655. (d) Johansson, H.; Shanks, D.; Engman, L.; Amorati, R.; Pedulli, G. F.; Valgimigli, L. *J. Org. Chem.* **2010**, *75*, 7535–7541. (e) Amorati, R.; Menichetti, S.; Mileo, E.; Pedulli, G. F.; Viglianisi, C. *Chem.—Eur. J.* **2009**, *15*, 4402–4410.
- (13) Berkowitz, J.; Ellison, J. B.; Gutman, D. *J. Phys. Chem.* **1994**, *98*, 2744–2765.
- (14) Denisov, E. *Handbook of Antioxidants*; CRC Press: Boca Raton, FL, 1995. Luo, Y.-R. *Comprehensive Handbook of Chemical Bond Energies*; CRC Press: Boca Raton, FL, 2007.
- (15) (a) Baciocchi, E.; Bietti, M.; Gerini, M. F.; Lanzalunga, O. *J. Org. Chem.* **2005**, *70*, 5144–5149. (b) Coseri, S.; Mendenhall, G. D.; Ingold, K. U. *J. Org. Chem.* **2005**, *70*, 4629–4636.
- (16) Avila, D. V.; Brown, C. E.; Ingold, K. U.; Luszyk, J. *J. Am. Chem. Soc.* **1993**, *115*, 466–470.
- (17) The PINO concentration in the LFP experiments is ca. 0.01 mM, phenol concentrations are in the range 0.05–4.5 mM.
- (18) (a) Das, P. K.; Encinas, M. V.; Steenken, S.; Scaiano, J. C. *J. Am. Chem. Soc.* **1981**, *103*, 4162–4166. (b) Shukla, D.; Schepp, N. P.; Mathivanan, N.; Johnston, L. J. *Can. J. Chem.* **1997**, *75*, 1820–1829.
- (19) Radical combination reactions of PINO are very fast ($k > 10^7 \text{ M}^{-1} \text{ s}^{-1}$), see: Koshino, N.; Saha, B.; Espenson, J. H. *J. Org. Chem.* **2003**, *68*, 9364–9370.
- (20) Nakanishi, I.; Fukuhara, K.; Shimada, T.; Ohkubo, K.; Iizuka, Y.; Inami, K.; Mochizuchi, M.; Urano, S.; Itoh, S.; Miyata, N.; Fukuzumi, S. *J. Chem. Soc., Perkin Trans. 2* **2002**, 1520–1524.
- (21) The rate constant for the hydrogen abstraction from PMC should be similar to that found in the reaction of $t\text{BuO}^\bullet$ with α -tocopherol, $k_{\text{H}} = 9.4 \times 10^8 \text{ M}^{-1} \text{ s}^{-1}$ in CH_3CN ,²² this value should be compared with the value of $k_{\text{H}} = 5.7 \times 10^7 \text{ M}^{-1} \text{ s}^{-1}$ for the hydrogen abstraction from NHPI by CumO^\bullet .²³
- (22) Valgimigli, L.; Banks, J. T.; Ingold, K. U.; Luszyk, J. *J. Am. Chem. Soc.* **1995**, *117*, 9966–9971.
- (23) Baciocchi, E.; Bietti, M.; Di Fusco, M.; Lanzalunga, O. *J. Org. Chem.* **2007**, *72*, 8748–8754.
- (24) Lucarini, M.; Pedrielli, P.; Pedulli, G. F.; Cabiddu, S.; Fattuoni, C. *J. Org. Chem.* **1996**, *61*, 9259–9263.
- (25) Brigati, G.; Lucarini, M.; Mugnaini, V.; Pedulli, G. F. *J. Org. Chem.* **2002**, *67*, 4828–4832.
- (26) Bordwell, F. G.; Cheng, J. P. *J. Am. Chem. Soc.* **1991**, *113*, 1736–1743.
- (27) Torres, E.; DiLabio, G. A. *J. Phys. Chem. Lett.* **2012**, *3*, 1738–1744. For tools to generate input files incorporating DCPs, see also www.ualberta.ca/~gdilabio.
- (28) Becke, A. D. *J. Chem. Phys.* **1993**, *98*, 5648–5652.
- (29) Lee, C.; Yang, W.; Parr, R. G. *Phys. Rev. B* **1988**, *37*, 785–789.
- (30) All calculations described herein were performed with the Gaussian-09 program package: Frisch, M. J.; Trucks, G. W.; Schlegel, H. B.; Scuseria, G. E.; Robb, M. A.; Cheeseman, J. R.; Scalmani, G.; Barone, V.; Mennucci, B.; Petersson, G. A. et al. *Gaussian 09*, revision C.01; Gaussian, Inc.: Wallingford, CT, 2009.
- (31) All molecule, radical and prereaction complexes were verified to only positive vibration frequencies, whereas transition state structures for hydrogen atom transfer possessed a single, imaginary vibration associated with the transfer of the H atom from the phenol to PINO.
- (32) (a) Sinnokrot, M. O.; Valeev, E. F.; Sherrill, C. D. *J. Am. Chem. Soc.* **2002**, *124*, 10887–10893. (b) Wheeler, S. *J. Am. Chem. Soc.* **2011**, *133*, 10262–10274.
- (33) Over binding may occur in radical-molecule complexes due to erroneous charge transfer. In such cases, the DFT method employed wrongly predicts the singly-occupied molecular orbital (SOMO) of the radical to lie lower in energy than highest-occupied molecular orbital (HOMO) of the molecule, which results in excess charge transfer and, therefore, excess Coulomb attraction between the species (ref: Johnson, E. R.; Salamone, M.; Bietti, M.; DiLabio, G. A. *J. Phys. Chem. A*, in press). We verified that this erroneous over-binding is not occurring in our systems because, according to our computational approach, the PINO SOMO lies higher in energy than the HOMO of the phenols.
- (34) We tested the M06–2X functional,³⁵ which is formulated to include dispersion-corrections, on the PINO+5 reaction. This method produced results that were consistent with those predicted using our B3LYP-DCP approach.
- (35) Zhao, Y.; Truhlar, D. G. *Theor. Chem. Acc.* **2008**, *120*, 215–241.
- (36) The 1.7 kcal/mol derives from O–H bond weakening due to steric repulsion between the OH and the *ortho* *t*-butyl groups.³⁷
- (37) Ingold, K. U.; Taylor, D. R. *Can. J. Chem.* **1961**, *39*, 471–480.
- (38) Pratt, D. A.; DiLabio, G. A.; Valgimigli, L.; Pedulli, G. F.; Ingold, K. U. *J. Am. Chem. Soc.* **2002**, *124*, 11085–11092.
- (39) (a) Wijtmans, M.; Pratt, D. A.; Valgimigli, L.; DiLabio, G. A.; Pedulli, G. F.; Porter, N. A. *Angew. Chem., Int. Ed.* **2003**, *42*, 4370–4373. (b) Pratt, D. A.; DiLabio, G. A.; Mulder, P.; Ingold, K. U. *Acc. Chem. Res.* **2004**, *37*, 334–340. (c) Wijtmans, M.; Pratt, D. A.; Brinkhorst, J.; Serwa, R.; Valgimigli, L.; Pedulli, G. F.; Porter, N. A. *J. Org. Chem.* **2004**, *69*, 9215–9223. (d) Shang, Y.-J.; Qian, Y.-P.; Liu, X.-D.; Dai, F.; Shang, X.-L.; Jia, W.-Q.; Liu, Q.; Fang, J.-G.; Zhou, B. *J. Org. Chem.* **2009**, *74*, 5025–5031.
- (40) In our previous study,⁹ it was proposed that the hydrogen transfer from the phenolic O–H to PINO involves a proton coupled electron transfer (PCET)⁴¹ rather than a classical hydrogen atom transfer (HAT) with the electron and the proton transferred through different orbitals, the O–H hydrogen transferred (as a proton) to a σ -lone pair on the PINO oxygen, whereas the electron is transferred from a p - π orbital on the phenol to the p singly occupied orbital on the PINO oxygen.
- (41) (a) Mayer, J. M.; Hrovat, D. A.; Thomas, J. L.; Borden, W. T. *J. Am. Chem. Soc.* **2002**, *124*, 11142–11147. (b) Mayer, J. M. *Annu. Rev. Phys. Chem.* **2004**, *55*, 363–390. (c) Rhile, I. J.; Mayer, J. M. *J. Am. Chem. Soc.* **2004**, *126*, 12718–12719. (d) Rhile, I. J.; Markle, T. F.; Nagao, H.; DiPasquale, A. G.; Lam, O. P.; Lockwood, M. A.; Rotter, K.; Mayer, J. M. *J. Am. Chem. Soc.* **2006**, *128*, 6075–6088.
- (42) (a) Bietti, M.; DiLabio, G. A.; Lanzalunga, O.; Salamone, M. J. *J. Org. Chem.* **2010**, *75*, 5875–5881. (b) Bietti, M.; DiLabio, G. A.; Lanzalunga, O.; Salamone, M. J. *J. Org. Chem.* **2011**, *76*, 1789–1794.
- (43) Howard, J. A.; Ingold, K. U. *Can. J. Chem.* **1963**, *41*, 2800–2806.
- (44) Calculated as ΔBDE values using the phenolic O–H BDEs listed in Table 1 and the value of 88.1 kcal mol⁻¹ for the NO–H BDE of NHPI.¹⁰
- (45) (a) Baciocchi, E.; Bietti, M.; Di Fusco, M.; Lanzalunga, O.; Raponi, D. *J. Org. Chem.* **2009**, *74*, 5576–5583. (b) Baciocchi, E.; Bietti, M.; D’Alfonso, C.; Lanzalunga, O.; Lapi, A.; Salamone, M. *Org. Biomol. Chem.* **2011**, *9*, 4085–4090.
- (46) (a) Baciocchi, E.; Bietti, M.; Lanzalunga, O.; Lapi, A.; Raponi, D. *J. Org. Chem.* **2010**, *75*, 1378. (b) Chamorro, E.; Bessolo, J.; Duque-Noreña, M.; Pérez, P. *Chem. Phys. Lett.* **2012**, *534*, 67–71.
- (47) Nakanishi, I.; Kawashima, T.; Ohkubo, K.; Kanazawa, H.; Inami, K.; Mochizuchi, M.; Kiyoshi, F.; Okuda, H.; Ozawa, T.; Itoh, S.; Fukuzumi, S.; Ikota, N. *Org. Biomol. Chem.* **2005**, *3*, 626–629.
- (48) With PMC the free energy change for electron transfer is positive ($\Delta G_{\text{et}}^0 = 0.28 \text{ V}$). In such a case, the overall rate of hydrogen

transfer (k_{H}) which consists of electron-transfer and proton-transfer steps would be lower than the initial electron-transfer rate (k_{et}). The maximum k_{et} value (ca. $2 \times 10^6 \text{ M}^{-1} \text{ s}^{-1}$) is evaluated from the ΔG_{et}^0 value ($k_{\text{et}} = Z \exp(\Delta G_{\text{et}}^0/k_{\text{B}}T)$, where Z is the frequency factor taken as $1 \times 10^{11} \text{ M}^{-1} \text{ s}^{-1}$, and k_{B} is the Boltzmann constant). The k_{H} value ($2.5 \times 10^8 \text{ M}^{-1} \text{ s}^{-1}$) is significantly larger than the k_{et} value thus indicating that the hydrogen transfer proceeds via a direct one-step HAT rather than via ET.

(49) Fukuzumi, S.; Tokuda, Y.; Chiba, Y.; Greci, L.; Carloni, P.; Damiani, E. *J. Chem. Soc., Chem. Commun.* **1993**, 1575–1577.

(50) It was possible to examine only a limited number of solvents, since in many cases there were problems related to the solubility of NHPI or to a very fast decay of the cumyloxyl radical.

(51) Abraham, M. H.; Grellier, P. L.; Prior, D. V.; Morris, J. J.; Taylor, P. J. *J. Chem. Soc., Perkin Trans. 2* **1990**, 521–529.

(52) (a) Snelgrove, D. W.; Lusztyk, J.; Banks, J. T.; Mulder, P.; Ingold, K. U. *J. Am. Chem. Soc.* **2001**, *123*, 469–477. (b) MacFaul, P. A.; Ingold, K. U.; Lusztyk, J. *J. Org. Chem.* **1996**, *61*, 1316–1321. (c) Avila, D. V.; Ingold, K. U.; Lusztyk, J.; Green, W. H.; Procopio, D. R. *J. Am. Chem. Soc.* **1995**, *117*, 2929–2930.

(53) Litwinienko, G.; Ingold, K. U. *Acc. Chem. Res.* **2007**, *40*, 222–230.

(54) Abraham, M. H.; Grellier, P. L.; Prior, D. V.; Duce, P. P.; Morris, J. J.; Taylor, P. J. *J. Chem. Soc., Perkin Trans. 2* **1989**, 699–711.

(55) Valgimigli, L.; Banks, J. T.; Lusztyk, J.; Ingold, K. U. *J. Org. Chem.* **1999**, *64*, 3381–3383.

(56) DiLabio, G. A.; Johnson, E. R. *J. Am. Chem. Soc.* **2007**, *129*, 6199–6203.

(57) Mayer, J. M. *Acc. Chem. Res.* **2011**, *44*, 36–46.

(58) Sutin, N. *Prog. Inorg. Chem.* **1983**, *30*, 441–498.

(59) Derived from pseudo-self-exchange reactions ($t\text{BuOO}\bullet + s\text{BuOOH}$). Chenier, J. H. B.; Howard, J. A. *Can. J. Chem.* **1975**, *53*, 623–627.

(60) Warren, J. J.; Mayer, J. M. *Proc. Natl. Acad. Sci.* **2010**, *107*, 5282–5287.

(61) Evans, M. G.; Polanyi, M. *Trans. Faraday Soc.* **1938**, *34*, 11–24. Most organic HAT processes typically have $|\Delta S^\ddagger| = 0$ because there is no change in the charges of the species involved and little change in their sizes.